Journal of The Electrochemical Society, **153** (6) A956-A960 (2006)
0013-4651/2006/153(6)/A956/5/$20.00 © The Electrochemical Society

Comparative Performance of Anode-Supported SOFCs Using a Thin $Ce_{0.9}Gd_{0.1}O_{1.95}$ Electrolyte with an Incorporated $BaCe_{0.8}Y_{0.2}O_{3-\alpha}$ Layer in Hydrogen and Methane

Atsuko Tomita,[a] Shinya Teranishi,[b,*] Masahiro Nagao,[b,*] Takashi Hibino,[b,,z] and Mitsuru Sano[b,**]**

[a]*National Institute of Advanced Industrial Science and Technology (AIST), Nagoya 463-8560, Japan*
[b]*Graduate School of Environmental Studies, Nagoya University, Nagoya 464-8601, Japan*

Multilayered $Ce_{0.9}Gd_{0.1}O_{1.95}/BaCe_{0.8}Y_{0.2}O_{3-\alpha}/Ce_{0.9}Gd_{0.1}O_{1.95}$ (GDC/BCY/GDC) electrolytes were prepared by tape casting on a Ni–$Ce_{0.8}Sm_{0.2}O_{1.9}$ anode support. The overall electrolyte thickness ranged from 30 to 35 μm, including a 3 μm thick BCY layer. When the multilayered electrolyte cell was tested with hydrogen at the anode and air at the cathode in the temperature range of 500–700°C, it yielded open-circuit voltages (OCVs) of 846–1024 mV, which were higher than the OCVs of 753–933 mV obtained for a single-layered GDC electrolyte cell under the same conditions. The corresponding peak power densities reached 273, 731, and 1025 mW cm^{-2} at 500, 600, and 700°C, respectively. The multilayered electrolyte cell could also be applied to direct methane solid oxide fuel cell (SOFC) and single-chamber SOFC operating in a mixture of methane and air. These SOFCs yielded OCVs of 880–950 mV and reasonable power densities without coking.
 [DOI: 10.1149/1.2186184]

Manuscript submitted November 25, 2005; revised manuscript received January 26, 2006. Available electronically April 6, 2006.

There has been considerable recent interest in solid oxide fuel cells (SOFCs) operating at intermediate temperatures of 700°C or less.[1] Compared with polymer electrolyte fuel cells (PEFCs), the intermediate-temperature solid oxide fuel cells (IT-SOFCs) can tolerate CO even at high concentrations and they can work with much higher electrode reaction rates.[2] Unlike conventional high-temperature SOFCs, the IT-SOFCs allow for the direct use of a hydrocarbon fuel, significantly reducing the complexity of the fuel-cell systems.[3,4] A key issue in the development of IT-SOFCs is the use of a highly ion conductive electrolyte, because the operation of SOFCs under such conditions results in excessive electrical resistance in the cell. Ceria-based oxide-ion conductors are promising electrolytes that exhibit much higher ion conductivities than yttria-stabilized zirconia (YSZ). Combined with advanced anode-supported cell structures, ceria-based SOFCs can maintain acceptable performance at intermediate temperatures.[5-13]

The primary problem encountered in using ceria-based electrolytes for IT-SOFCs is the partial reduction of ceria in fuel atmospheres.[14] This results in n-type electronic conductivity, causing partial internal electronic short circuits in the cell. It also results in expansion of the crystal lattice, leading to mechanical degradation inside the electrolyte or at the electrolyte-electrode interface. Therefore, ceria-based SOFCs must be processed at temperatures below 500°C, where the reduction of ceria is thermodynamically suppressed.[15]

We recently proposed an effective approach to avoid partial reduction of ceria.[16,17] The surface of a Sm^{3+}- or Gd^{3+}-doped ceria substrate with a thickness of 0.5 mm was coated with a thin BaO film and then heated up to 1500°C. Consequently, a solid-state reaction between the film and the substrate formed a ~10 μm thick $BaCe_{1-x}Sm_x$(or Gd_x)$O_{3-\alpha}$ layer on the substrate surface. Using the coated electrolyte, a hydrogen-air SOFC showed open-circuit voltages (OCVs) above 1 V in the temperature range of 600–950°C. The intermediate layer also showed strong bonding with the electrolyte substrate, allowing no delamination and cracking of the layer. This is an important advantage over other techniques which typically involve depositing a thin YSZ film on ceria-based electrolytes by room temperature sputtering, ion plating, or sol-gel coating.[18-20] However, in principle, it is difficult to apply our method to anode-supported SOFCs because we cannot form the intermediate layer during the growth of the electrolyte film on the anode substrate. In addition, an insulator, such as $BaNiO_3$, may simultaneously form at the anode-electrolyte interface.

In this study, we attempted to improve the above method by inserting a previously prepared $BaCeO_3$-based layer between two ceria-based electrolyte films. Tape casting is one of the most widely used techniques for making laminated materials.[21] This technique allowed for the preparation of a high-quality multilayered electrolyte on the anode substrate. $BaCe_{0.8}Y_{0.2}O_{3-\alpha}$ and $Ce_{0.9}Gd_{0.1}O_{1.95}$ were chosen as the intermediate layer material and the electrolyte due to high reduction resistance[22] and high ion conductivity,[14] respectively. SOFCs with the multilayered electrolyte were tested with hydrogen and methane in the temperature range of 400–700°C. The feasibility of applying the multilayered electrolyte cells to single-chamber SOFCs (Refs. 23-28) was also evaluated.

Experimental

Anode powders of NiO, $Ce_{0.8}Sm_{0.2}O_{1.9}$ (SDC, Anan Kasei), and acetylene black in proportions of 47.5, 47.5, and 5.0 wt %, respectively, were ground in a mixture of isopropanol (as solvent), a small amount of pridine (as dispersant) and adipic acid (as plasticizer) using a planetary ball mill for 24 h. Then, 30.0 wt % of polyvinyl-butiral resin was added as binder. The mixture was again ball-milled for 24 h to form a homogeneous suspension. This suspension was cast on a stationary PET foil using a doctor blade with a slit width of 0.4 mm. After drying at 110°C, the anode tape was carefully removed from the foil and cut into 20 sheets, each with a thickness of 100 μm.

Single- and multilayered electrolyte tapes were prepared in a similar manner to the above procedure. However, in the case of the multilayered tapes, the suspensions were cast layer-by-layer in the order of $Ce_{0.9}Gd_{0.1}O_{1.95}$ (GDC, Anan Kasei), $BaCe_{0.8}Y_{0.2}O_{3-\alpha}$ (BCY, Anan Kasei), and GDC suspensions. The thickness of the green GCD layer was fixed at a value of 20 μm, and that of the green BCY layer was varied in the range of 2–10 μm by adjusting the slit width of the blade. An electrolyte sheet was obtained by taking the tape off the substrate foil and cutting it into a suitable size.

One electrolyte and 20 anode sheets were laminated by warm pressing at 90°C for 15 s. The laminated sample was heated up to 500°C and held for 2 h to remove all organic additives. Final sintering was carried out at 1350°C for 5 h. The dimensions of the sintered composite ceramic were approximately 12 × 12 × 1.5 mm. Microstructures of the ceramic material were observed by scanning electron microscopy (SEM).

Homemade $Sm_{0.5}Sr_{0.5}CoO_3$ (thickness about 10 μm, area

* Electrochemical Society Student Member.
** Electrochemical Society Active Member.
z E-mail: hibino@urban.env.nagoya-u.ac.jp

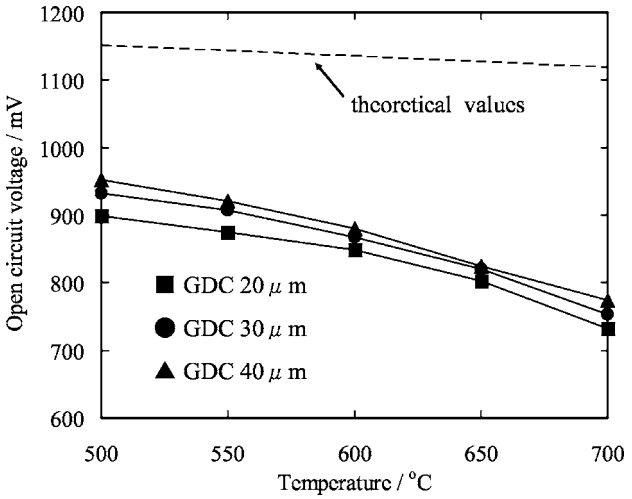

Figure 1. OCV vs operating temperature of SOFCs with 20–40 μm thick GDC electrolytes operating on hydrogen.

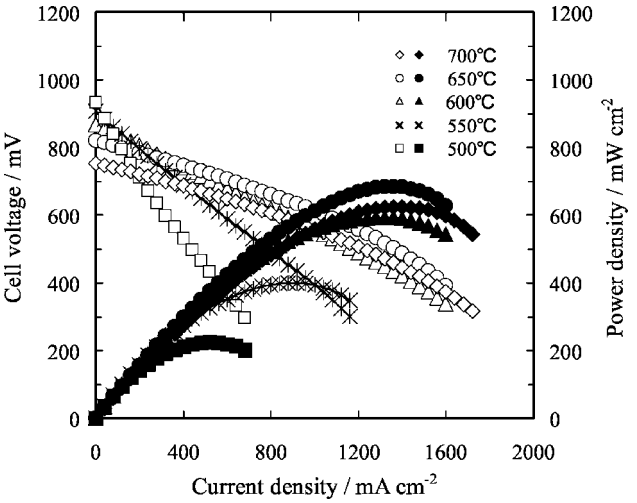

Figure 2. Cell voltage and power density vs current density of SOFC with a 30 μm thick GDC electrolyte for hydrogen.

0.5 cm^2) was used as the cathode for the fuel-cell tests. The preparation and treatment of this material is described in detail elsewhere.[23,28] Two kinds of fuel-cell configurations, dual-chamber and single-chamber fuel cells, were tested in this study. The dual-chamber fuel cell was fabricated by placing the cell assembly between two alumina tubes. The anode chamber was sealed by melting a glass ring gasket at 950°C. Electrical collection for the cell was performed using a Au mesh for the anode and a Pt mesh for the cathode. The anode chamber was supplied with wet hydrogen, saturated with H_2O vapor at room temperature, and unhumidified methane at a flow rate of 30 mL min^{-1}. The cathode chamber was exposed to atmospheric air. The single-chamber fuel cell was set up in an alumina tube. The Pt mesh was used as the electrical collector for the anode, and the Au mesh was similarly used for the cathode. A mixture of methane and air with a methane-to-oxygen ratio of 2 was supplied to the cell at a flow rate of 300 mL min^{-1}. Fuel-cell tests were performed by measuring the current-voltage curves during discharge of the cell using a galvanostat (Hokuto Denko HA-501) and by measuring the impedance spectrum under open-circuit conditions using an impedance analyzer (Solartron SI-1260). These measurements were conducted using a four-probe method.

Results and Discussion

Single-layered GDC electrolyte films.— The performance of SOFCs with different thicknesses of single-layered GDC electrolyte was first measured in the temperature range of 500–700°C. Figure 1 shows typical plots of the OCVs as a function of the operating temperature, with hydrogen at the anode and air at the cathode. The measured OCV values were 22.5–25.3% lower than the theoretical values (Nernst potentials) for these conditions. The validity of this result is confirmed by comparison with experimental data reported[5-13] (see Table I). All the listed OCV values are about 850 mV at 600°C, which are close to the OCV values (849–880 mV) under similar conditions shown in Fig. 1. Therefore, the differences between the measured and theoretical OCVs shown in Fig. 1 can be attributed to the reduction of ceria in fuel conditions rather than physical leakage of gas through the present electrolyte films. It can also be observed in Fig. 1 that the improvement in OCV by increasing the electrolyte thickness from 20 to 40 μm was only a few decades of mV. This process simultaneously increased the electrical resistance of the SOFC from 0.18 to 0.39 Ω cm^2. Thus, increasing the electrolyte thickness is not a useful method for improving the OCV of ceria-based SOFCs.

The cell voltage and power density versus the current density of the 30 μm GDC electrolyte cell operating on hydrogen are shown in Fig. 2. A peak power density of 593 mW cm^{-2} at 600°C was comparable to or higher than the values summarized in Table I, indicating that the electrical resistance of the present electrolyte is a reasonable value. Figure 2 also shows that the dependence of the peak power density on the operating temperature was very small above 600°C. This can be explained because the reduced OCV of the SOFC at high temperatures compensates for the decrease in potential drop with increasing temperature. Another possible explanation is the expansion of the crystal lattice by excessive reduction of ceria that leads to mechanical failure of the cell. This explanation is especially valid at 700°C because the electrical resistance at this temperature was slightly higher than that at 650°C.

Multilayered GDC/BCY/GDC electrolyte films.— In an attempt to suppress the reduction of ceria, a thin BCY layer was inserted between the GDC electrolyte films. As can be seen from the cross-sectional image in Fig. 3, the overall electrolyte thickness ranged

Table I. Performances of various anode-supported SOFCs with ceria-based electrolytes at 600°C.

Electrolyte	Thickness (μm)	Anode	Cathode	OCV (mV)	Peak power density (mW cm^{-2})	Literature
$Ce_{0.85}Sm_{0.15}O_{1.925}$	20	Ni-SDC (60:40)	$Ba_{0.5}Sr_{0.5}Co_{0.8}Fe_{0.2}O_{3-\alpha}$	ca. 850	1010	Ref. 5
$Ce_{0.8}Gd_{0.2}O_{1.9}$	10	Ni-SDC (65:35)	$La_{0.8}Sr_{0.2}Co_{0.2}Fe_{0.8}O_3$	863	578	Ref. 8
$Ce_{0.9}Gd_{0.1}O_{1.95}$	20	Ni-SDC (65:35)	$Sm_{0.5}Sr_{0.5}CoO_3$	852	602	Ref. 7
$Ce_{0.9}Gd_{0.1}O_{1.95}$	26	Ni-SDC (65:35)	$Sm_{0.5}Sr_{0.5}CoO_3$	ca. 850	270	Ref. 10
$Ce_{0.8}Sm_{0.2}O_{1.9}$	30	Ni-SDC (65:35)	$Sm_{0.5}Sr_{0.5}CoO_3$	ca. 850	397	Ref. 6
$Ce_{0.8}Y_{0.2}O_{1.9}$	15	Ni-SDC (65:35)	$Sm_{0.5}Sr_{0.5}CoO_3$	ca. 860	230	Ref. 9
$Ce_{0.8}Sm_{0.2}O_{1.9}$	25	Ni-SDC (50:50)	$Sm_{0.5}Sr_{0.5}CoO_3$	880	491	Ref. 11
$Ce_{0.9}Gd_{0.1}O_{1.95}$	35	$Fe_{0.25}Co_{0.25}Ni_{0.5}$-SDC	$Sm_{0.5}Sr_{0.5}CoO_3$	820	750	Ref. 12

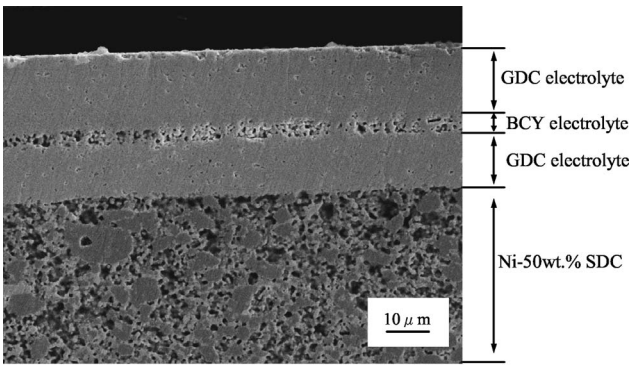

Figure 3. SEM cross-sectional micrograph of GDC/BCY/GDC electrolyte. The thickness of the BCY layer was 3 μm.

from 30 to 35 μm, including an approximately 3 μm thickness of the BCY layer. The GDC layers on both the anodic and cathodic sides were sufficiently dense to prohibit crossover of gases through the layer, while the BCY layer showed relatively poor density, probably due to the difference in the thermal expansion between the GDC and BCY phases; the thermal expansion coefficients of GDC and BCY were 11.9×10^{-6} and 11.08×10^{-6} K^{-1}, respectively. It is clear that the quality of the BCY layer hereafter needs to be improved.

Figure 4 shows the OCVs of the SOFCs with the multilayered GDC/BCY (thickness 1, 3, and 5 μm)/GDC electrolytes as a function of the operating temperature, with hydrogen at the anode and air at the cathode. Disregarding the poor density of the BCY layer, the use of the GDC/BCY/GDC electrolyte increased the OCV value by 30–180 mV, depending on the thickness of the BCY layer and on the operating temperature. The increment in OCV became larger with increasing layer thickness and temperature. Figure 4 also shows the OCVs of the SOFC with a 30 μm thick single-layered BCY electrolyte for comparison. The measured OCV exceeded 1 V over the whole temperature range of interest, although slightly lower than the theoretical values (1.16 to 1.19 V at 500 to 700°C). This indicates that the BCY electrolyte could block the electronic current, and a similar effect is applicable to the BCY layer incorporated between the GDC electrolyte films for improvement of the OCV.

The overall electrical resistances of the SOFCs with the three GDC/BCY/GDC electrolytes described above operating with hydrogen at 600°C are given in Table II, including the resistances of the SOFCs with the 30 μm thick GDC and 30 μm thick BCY electrolytes for comparison. A comparable resistance for the GDC/BCY/GDC and GDC electrolytes was achieved when the BCY layers were 1 and 3 μm thick. The optimal thickness of the BCY layer was thus determined to be 3 μm based on the criteria for keeping the OCV as high as possible and the resistance as low as possible. The BCY electrolyte cell showed a resistance of 28.58 Ω cm^2, which is much higher than the resistance of 0.45 Ω cm^2 expected for ionic conductivity.[22] This is likely due to the formation of reaction products with low conductivities at the electrolyte-anode interface, as well as poor electrode kinetics.

Table II. Internal electrical resistances of anode-supported SOFCs with single-layered GDC and BCY electrolytes and multilayered GDC/BCY/GDC electrolytes at 600°C

		GDC/BCY/GDC electrolyte			
	GDC electrolyte /30 μm	BCY 1 μm	BCY 3 μm	BCY 5 μm	BCY electrolyte /30 μm
Electrical resistances /Ω cm^2	0.27	0.29	0.31	0.61	28.58

The performance of the SOFC with the GDC/BCY/GDC electrolyte in the temperature range of 500–700°C is shown in Fig. 5. Compared with the power density of the GDC electrolyte cell shown in Fig. 2, higher power densities were generated from the GDC/BCY/GDC electrolyte cell at all tested temperatures. This is mainly attributable to enhanced OCV by the insertion of the BCY layer between the GDC electrolyte films. It is also possible that the mechanical properties of the electrolyte are improved by suppressing excessive reduction of ceria. Indeed, the electrical resistance of the GDC/BCY/GDC electrolyte cell decreased with increasing temperature from 500 to 700°C, which is different from the behavior observed for the GDC electrolyte cell, as described in the previous section.

Comparison of power densities for a cell voltage of 700 mV between the above two SOFCs further emphasizes the advantages of the GDC/BCY/GDC electrolyte over the GDC electrolyte. The results are shown in Fig. 6, where both cells were operated under the same conditions. The performance of the GDC/BCY/GDC electrolyte cell was higher than that of the GDC electrolyte cell at all tested temperatures. In addition, the power density of the GDC/BCY/GDC electrolyte SOFC was enhanced with increasing temperature, while

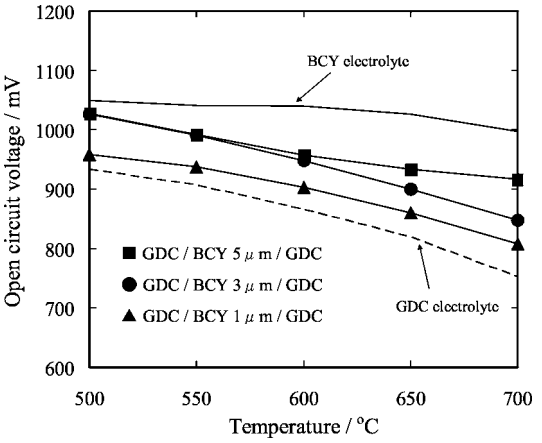

Figure 4. OCV vs operating temperature of SOFCs with GDC/BCY/GDC electrolytes for hydrogen. The thickness of the BCY layer was 1, 3, and 5 μm.

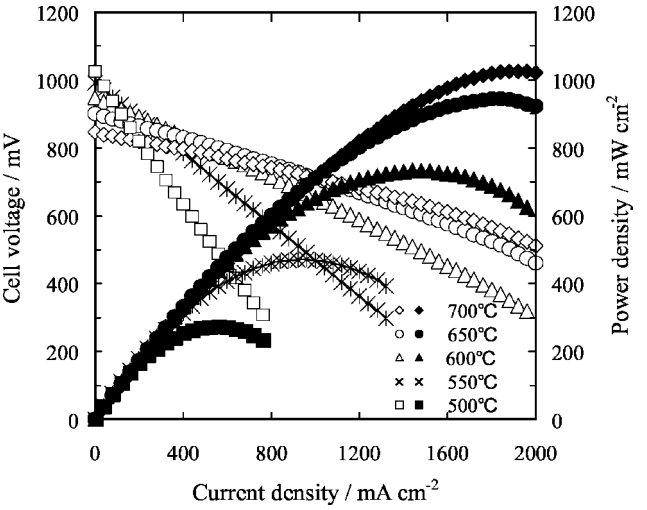

Figure 5. Cell voltage and power density vs current density of an SOFC with GDC/BCY/GDC electrolyte for hydrogen. The thickness of the BCY layer was 3 μm.

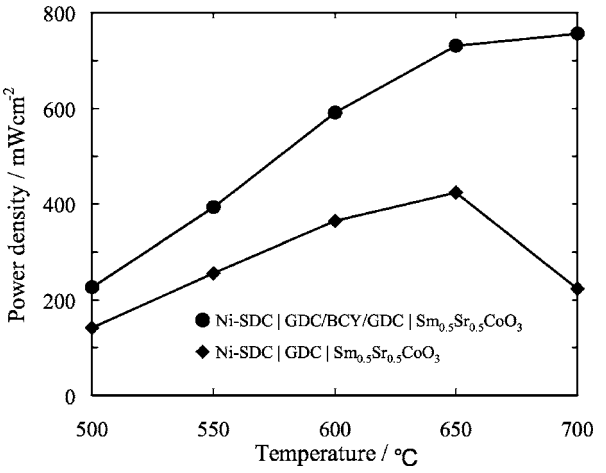

Figure 6. Power density at 0.7 V vs operating temperature of SOFCs with 30 μm thick GDC electrolyte and GDC/BCY/GDC electrolyte for hydrogen. The thickness of the BCY layer was 3 μm.

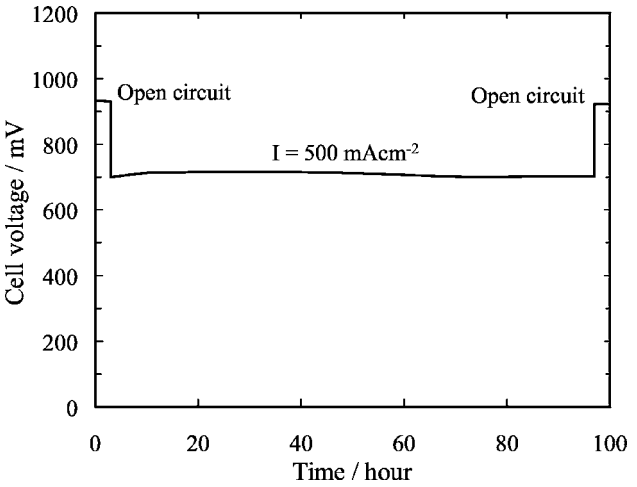

Figure 8. Cell voltage at a constant current density of 500 mA cm^{-2} vs operating time. The experiment was conducted at 600°C.

that of the GDC electrolyte SOFC was suddenly reduced at 700°C. It is thus concluded that the insertion of the BCY layer between the GDC electrolyte films is a promising method to enhance the performance of ceria-based SOFCs and their stability in hydrogen atmospheres.

Direct methane SOFC and single-chamber SOFC with multilayer GDC/BCY/GDC electrolyte film.— An additional objective of this study was to demonstrate the feasibility of using the multilayered GDC/BCY/GDC electrolyte as the electrolyte for SOFCs with hydrocarbon fuels at intermediate temperatures. Two types of SOFCs were fabricated with the GDC/BCY/GDC electrolyte: a direct methane SOFC and a single-chamber SOFC operating in a mixture of methane and air.

Using the same SOFC used in the previous section, the anode chamber was supplied with unhumidified methane instead of hydrogen. Figure 7 shows the cell voltage and power density as a function of the current density of the SOFC operating with methane in the temperature range of 500–650°C. The multilayered electrolyte cell yielded OCV values for methane close to the values for hydrogen shown in Fig. 5. However, the peak power densities were lower for methane (611 mW cm^{-2} at 600°C as an example) than for hydrogen (731 mW cm^{-2} at 600°C), suggesting that the electrochemical reaction is slower for methane than for hydrogen. Figure 8 shows the cell voltage at a constant current density of 500 mA cm^{-2} as a function of time at 600°C. The cell voltage was very stable during an 80 h test using methane fuel, indicating that carbon deposition on the anode is minimal for at least 80 h. Similar results have been reported by Barnett et al.,[3,29] who explain the carbon-free operation as due to the relatively lower rate of methane cracking than the rate of methane oxidation at temperatures below 700°C.

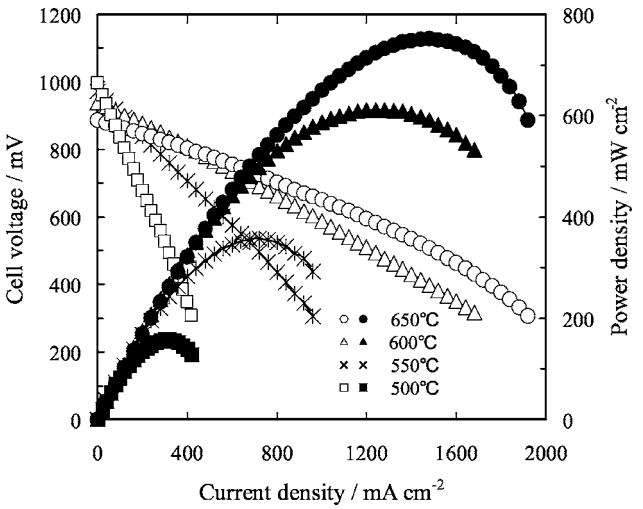

Figure 7. Cell voltage and power density vs current density of direct methane SOFC with GDC/BCY/GDC electrolytes. The thickness of the BCY layer was 3 μm.

The whole SOFC was placed in an alumina tube and then supplied with a mixture of methane and air (methane-to-oxygen ratio = 2). It was difficult for the SOFC to operate at a furnace temperature above 550°C, at which the OCV could not reach a value higher than 300 mV. In general, the operation of the single-chamber SOFC is based on the difference in catalytic activity for the partial oxidation of methane between the two electrode materials.

$$CH_4 + 1/2\ O_2 \rightarrow CO + 2H_2 \qquad [1]$$

This reaction proceeds to form hydrogen and carbon monoxide over the anode, whereas such an oxidation proceeds at a very slow rate over the cathode.[23-28] Therefore, the SOFC can yield a large OCV in the gas mixture. In the present case, the Ni-SDC anode, including the Pt mesh, showed high catalytic activity for the partial oxidation of methane. However, the $Sm_{0.5}Sr_{0.5}CoO_3$ cathode unfortunately functioned as an active catalyst for methane oxidation above 550°C. This is a reason for the low OCV observed. Upon decreasing temperature to 500°C or less, OCVs higher than 900 mV could be generated from the SOFC, as shown in Fig. 9. As a result, peak power densities of 302, 296, and 231 mW cm^{-2} were achieved at furnace temperatures of 500, 450, and 400°C, respectively. The small difference in power density between 500 and 450°C is likely because methane was still oxidized to some extent by the $Sm_{0.5}Sr_{0.5}CoO_3$ cathode at 500°C. Here, some care must be taken in understanding the performance of the single-chamber SOFC, because there is a large difference between the furnace temperature and actual cell temperature, due to reaction heat produced by the partial oxidation of methane.[24,30] We confirmed that the actual cell temperature rose by 150–200°C.

Finally, durability of the single-chamber SOFC was tested at a furnace temperature of 450°C. As shown in Fig. 10, the cell voltage for a current density of 450 mA cm^{-2} was slightly improved for an initial 5 h and was then maintained at an almost constant value of 620 mV. In addition, no carbon was observed after a 40 h test. This is in agreement with the results reported previously for single-chamber SOFCs for various hydrocarbon-air mixtures.[23-28] Another important point in the present results along with the results shown in

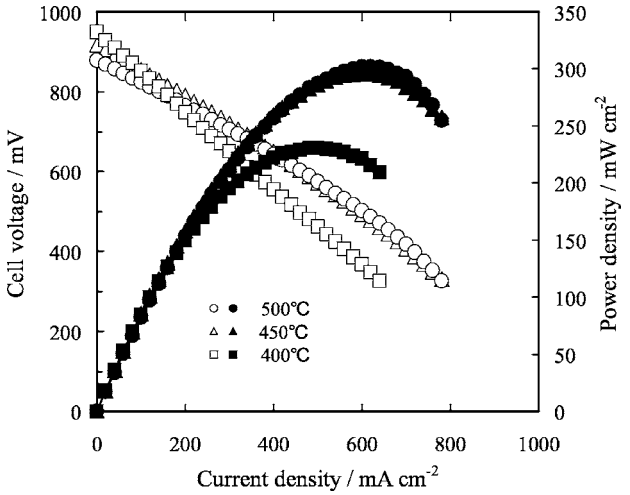

Figure 9. Cell voltage and power density vs current density of single-chamber SOFC with GDC/BCY/GDC electrolytes. The thickness of the BCY layer was 3 μm.

Fig. 8 is that stable performance of the multilayered electrolyte cell could be achieved in the presence of a large amount of carbon dioxide formed by discharging the cell, which suggests that the present electrolyte shows high chemical stability to carbon dioxide.

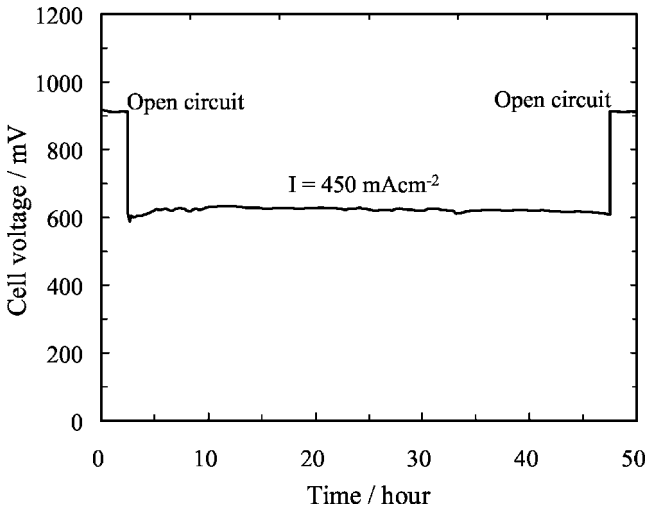

Figure 10. Cell voltage at a constant current density of 450 mA cm^{-2} vs operating time. The experiment was conducted at a furnace temperature of 450°C.

Conclusions

The present results showed that a BCY layer incorporated between GDC electrolyte films could block the electronic current through the cell. No formation of reaction products with low conductivity was observed at the layer-electrolyte interface. As a result, the multilayered GDC/BCY/GDC electrolyte cell yielded higher OCVs and power densities in the temperature range of 500–700°C than the single-layered GDC electrolyte cell. Moreover, the multilayered electrolyte cell could be operated directly with methane and a methane-air mixture, which is a major advantage for developing practical SOFC applications.

Nagoya University assisted in meeting the publication costs of this article.

References

1. B. C. H. Steele and A. Heinzel, *Nature (London)*, **414**, 345 (2001).
2. B. C. H. Steele, *Solid State Ionics*, **129**, 95 (2000).
3. E. P. Murray, T. Tsai, and S. A. Barnett, *Nature (London)*, **400**, 649 (1999).
4. S. Park, J. M. Vohs, and R. J. Gorte, *Nature (London)*, **404**, 265 (2000).
5. Z. Shao and S. M. Haile, *Nature (London)*, **431**, 170 (2004).
6. C. Xia, F. Chen, and M. Liu, *Electrochem. Solid-State Lett.*, **4**, A52 (2001).
7. S. Zha, A. Moore, H. Abernathy, and M. Liu, *J. Electrochem. Soc.*, **151**, A1128 (2004).
8. Y. J. Leng, S. H. Chan, S. P. Jiang, and K. A. Khor, *Solid State Ionics*, **170**, 9 (2004).
9. R. Peng, C. Xia, X. Liu, D. Peng, and G. Meng, *Solid State Ionics*, **152–153**, 561 (2002).
10. C. Xia and M. Liu, *Solid State Ionics*, **144**, 249 (2001).
11. Y. Yin, W. Zhu, C. Xia, and G. Meng, *J. Power Sources*, **36**, 132 (2004).
12. Z. Xie, W. Zhu, B. Zhu, and C. Xia, *Electrochim. Acta*, to be published.
13. T. Hibino, A. Hashimoto, M. Yano, M. Suzuki, and M. Sano, *Electrochim. Acta*, **48**, 2531 (2003).
14. V. V. Khartona, F. M. B. Marquesa, and A. Atkinson, *Solid State Ionics*, **174**, 135 (2004).
15. R. Doshi, R. Von L. Richards, J. D. Carter, X. Wang, and M. Krumpelt, *J. Electrochem. Soc.*, **146**, 1273 (1999).
16. D. Hirabayashi, A. Tomita, T. Hibino, M. Nagao, and M. Sano, *Electrochem. Solid-State Lett.*, **7**, A318 (2004).
17. D. Hirabayashi, A. Tomita, S. Teranishi, T. Hibino, and M. Sano, *Solid State Ionics*, **176**, 881 (2005).
18. K. Eguchi, T. Setoguchi, T. Inoue, and H. Arai, *Solid State Ionics*, **90**, 165 (1992).
19. K. Mehta, S. J. Hong, J. F. Jue, and A. V. Virkar, in Proceedings of the 3rd International Symposium on Solid Oxide Fuel Cells, S. C. Singhal and H. Iwahara, Editors, PV 93-4, p. 92, The Electrochemical Society Proceedings Series, Pennington, NJ (1993).
20. S. G. Kim, S. P. Yoon, S. W. Nam, S. H. Hyun, and S. A. Hong, *J. Power Sources*, **110**, 222 (2002).
21. D. Hotza and P. Greil, *Mater. Sci. Eng., A*, **202**, 206 (1995).
22. T. Hibino, A. Hashimoto, M. Suzuki, and M. Sano, *J. Electrochem. Soc.*, **149**, A1503 (2002).
23. T. Hibino, A. Hashimoto, T. Inoue, J. Tokuno, S. Yoshida, and M. Sano, *Science*, **288**, 2031 (2000).
24. T. W. Napporn, F. Morin, and M. Meunier, *Electrochem. Solid-State Lett.*, **7**, A60 (2004).
25. T. Suzuki, P. Jasinski, V. Petrovsky, H. U. Anderson, and F. Dogan, *J. Electrochem. Soc.*, **151**, A1473 (2004).
26. S. Asahara, D. Machiba, M. Hibino, and T. Yao, *Electrochem. Solid-State Lett.*, **8**, A449 (2005).
27. B. E. Buergler, M. E. Siegrist, and L. J. Gauckler, *Solid State Ionics*, **176**, 1717 (2005).
28. A. Tomita, D. Hirabayashi, T. Hibino, M. Nagao, and M. Sano, *Electrochem. Solid-State Lett.*, **8**, A63 (2005).
29. Y. Lin, Z. Zhan, J. Liu, and S. A. Barnett, *Solid State Ionics*, **176**, 1827 (2005).
30. T. Hibino, A. Hashimoto, T. Inoue, J. Tokuno, S. Yoshida, and M. Sano, *J. Electrochem. Soc.*, **148**, A544 (2001).